

Parametric Down-Conversion of X Rays into the Optical Regime

A. Schori,¹ C. Bömer,² D. Borodin,¹ S. P. Collins,³ B. Detlefs,⁴ M. Moretti Sala,⁴ S. Yudovich,¹ and S. Shwartz^{1,*}

¹*Physics Department and Institute of Nanotechnology, Bar Ilan University, Ramat Gan, 52900 Israel*

²*European XFEL, Holzkoppel 4, 22869 Schenefeld, Germany*

³*Diamond Light Source, Harwell Science and Innovation Campus, Didcot OX11 0DE, United Kingdom*

⁴*European Synchrotron Radiation Facility, BP 220, F-38043 Grenoble Cedex, France*

(Received 21 August 2017; published 21 December 2017)

We report the observation of parametrically down-converted x-ray signal photons at photon energies that correspond to idler photons at optical wavelengths. The count-rate dependence on the angles of the input beam and of the detector and on the slit sizes agrees with theory within the experimental uncertainties. The nonlinear susceptibility, which we calculated from the measured efficiencies, is comparable to the nonlinear susceptibility evaluated from the measurements of x-ray and optical wave mixing. The results of the present Letter advance the development of a spectroscopy method for probing valence-electron charges and the microscopic optical response of crystals with atomic-scale resolution.

DOI: 10.1103/PhysRevLett.119.253902

Nonlinear interactions of x rays and optical radiation can provide insight into the microscopic structure of chemical bonds, the valence electron density of crystals, and light-matter interactions at the atomic-scale resolution [1–11]. The high resolution stems from the short wavelengths of x rays, whereas the optical fields interact with the valence electrons. This probe has great potential in the study of microscopic optical properties of materials. Unfortunately, the experimental realization of these ideas is very challenging, and only a few experiments in this direction have been reported [3–10] since they were proposed almost 50 years ago [1]. The experimental observation of parametric down-conversion (PDC) of x rays to optical wavelengths has never been reported.

In processes such as x-ray and optical sum-frequency generation (SFG) and difference-frequency generation (DFG), x rays and optical waves are mixed to generate an x-ray wave at a frequency that is equal to the sum or difference of the two input frequencies, respectively. The physical mechanism that supports the wave-mixing effect can be viewed as an inelastic scattering of the input x rays from an optically modulated charge density [2,5,11,12]. Glover and colleagues reported the first observation of x-ray and optical wave mixing in a diamond crystal by using an x-ray free-electron laser and a Ti-Sapphire laser [5]. The main challenge in observing SFG in other materials is the low efficiency, which depends linearly on the intensity of the optical laser. Consequently, the observation of the effect requires optical intensities that are larger than the radiation damage threshold of most materials. It is also clear that SFG can be observed only in optically transparent materials; thus, it is not applicable for a large class of materials such as metals and superconductors.

It is possible to overcome these challenges by using PDC of x rays to optical wavelengths. This nonlinear process is

similar to x-ray and optical DFG, but in x-ray to optical PDC, the pump photons interact with vacuum fluctuations to generate correlated x-ray and optical photon pairs [1].

It should be noted that the pertinent effect of x rays into extreme ultraviolet (EUV) PDC has been applied already to investigate the optical properties of crystals [3,4,6–10]. By using this approach, the microscopic linear susceptibility of a diamond crystal with a resolution of 0.54 Å has been extracted from the measurements of the PDC for several atomic planes [4]. The extension of that method to PDC of x rays to optical wavelengths could lead to a more powerful probe. For example, it could be utilized for the investigation of phenomena that are associated with energies near the Fermi energy of metals or near the band gap of semiconductors. However, the observation of this effect is even more challenging. This is because the photon energies of the generated x-ray signal differ by only a few eV from the photon energies of the pump and because the Bragg condition is very close to the phase-matching requirement of the PDC process. Since Bragg scattering is many orders of magnitude stronger than the PDC process, the tail of the Bragg scattering has to be filtered out stringently. This requires a highly collimated and monochromatic input beam and a careful design of the experimental setup.

In this Letter, we describe measurements of the x-ray signal generated during the process of PDC for idler photons at optical wavelengths. We use a highly collimated monochromatic beam and a high-resolution multibounce crystal analyzer to measure PDC at energies that correspond to various optical wavelengths in the range of 280–650 nm for several phase-matching conditions. We evaluate the nonlinear susceptibility from the measured efficiencies and find a reasonable agreement with the theory and with the results of SFG [5].

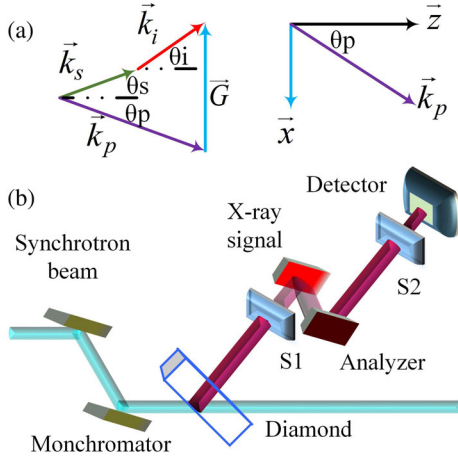


FIG. 1. (a) Phase-matching scheme. The indices p , s , and i represent the pump, signal, and idler, respectively; \vec{G} is the reciprocal lattice vector; and the angles θ_p , θ_s , and θ_i are the angles with respect to the atomic planes of the pump, the signal, and the idler, respectively. (b) Schematic of the experimental setup. The scattering plane of the analyzer is normal to the scattering plane of the diamond. S_1 and S_2 are the slits before the analyzer and before the detector, respectively.

Since x-ray wavelengths are comparable to the distance between the atomic planes, we use the reciprocal lattice vector for phase matching [12,13], as we depict in Fig. 1(a). In this Letter, we refer to the x-ray photons as the signal photons and to the optical photons as the idler photons. We denote θ_p , θ_s , and θ_i as the angles with respect to the atomic planes of the pump, the signal, and the idler, respectively. The k vectors of the pump, the signal, and the idler are \vec{k}_p , \vec{k}_s , and \vec{k}_i , respectively. Note that \vec{G} is the reciprocal lattice vector orthogonal to the atomic planes. The energy conservation implies that $\omega_p = \omega_s + \omega_i$, where we denote ω_p , ω_s , and ω_i as the angular frequencies of the pump, the signal, and the idler, respectively. The phase-matching condition can be written as $\vec{k}_p + \vec{G} = \vec{k}_s + \vec{k}_i$. Since the idler k vector is much smaller than the k vectors of the pump and the signal, the phase-matching angles of the PDC x-ray signal are very close to the Bragg angle. Consequently, the tail of the elastic scattering is not negligible, and the separation of the PDC x-ray signal from the elastic requires narrow filters for energy resolution and slits for angular resolution.

Under the assumptions of undepleted pump approximation, lossless medium, and slowly varying envelope approximation (SVEA), the coupled wave equations describing the PDC process in the frequency domain can be described as [13–15]

$$\begin{aligned} \frac{\partial a_s}{\partial z} &= -\kappa a_i^+ \exp[i\Delta k_z z], \\ \frac{\partial a_i^+}{\partial z} &= -\kappa^* a_s \exp[-i\Delta k_z z]. \end{aligned} \quad (1)$$

Here, a_s , a_i are signal and idler annihilation operators, $\Delta k_z = k_p \cos \theta_p - k_s \cos \theta_s - k_i \cos \theta_i$ is the phase mismatch, and $\kappa = [(2\hbar\eta_p\eta_s\eta_i\omega_p\omega_s\omega_i)^{\frac{1}{2}} J_s^{NL} / 2\omega_s E_i^* \sqrt{\cos \theta_s \cos \theta_i}]$ is the nonlinear interaction coefficient. We denote η_p , η_s , and η_i as the impedances at the pump, the signal, and the idler frequencies, respectively; \hbar is the reduced Planck constant; E_i is the electric field of the idler; and J_s^{NL} is the nonlinear current density.

The signal count rate is given by

$$R = \iint \kappa^2 \frac{\cos \theta_s \omega_s^2 \sin^2(\frac{1}{2} \Delta k_z z)}{(2\pi)^3 c^2 (\frac{1}{2} \Delta k_z z)^2} d\Omega d\omega_s, \quad (2)$$

where c is the speed of light in vacuum. The signal count rate is calculated numerically, where the integration is taken over the solid angle of the detector and the bandwidth of the analyzer. We note that the acceptance angle of the detector restricts the bandwidth due to the one-to-one relation between the angle of propagation and the wavelength of the generated x-ray signal, which is imposed by the requirement for exact phase matching in the directions parallel to the surface of the crystal.

We conducted the experiments described below at beam line ID-20 of the European Synchrotron Radiation Facility and at beam line I16 of Diamond Light Source [16]. The schematic of the experimental system is shown in Fig 1(b). The average input power is $\sim 1 \times 10^{13}$ photons/s and its polarization is horizontal. The nonlinear crystal is a diamond crystal with dimensions 4 mm \times 4 mm \times 0.8 mm, and the scattering plane is horizontal. We use the reciprocal lattice vector normal to the C(220) atomic planes in a Laue geometry to achieve the phase-matching condition. We use a multibounce Si crystal analyzer and two variable slits in front of and behind the analyzer, which we denote as S_1 and S_2 , to filter out the tail of the elastic diffraction. The analyzer scattering plane is in the vertical direction, which is normal to the scattering plane of the diamond crystal. We measure the PDC x-ray signal with an avalanche photo-diode. All experimental data are corrected for relative intensity fluctuations via measurements from a reference detector positioned upstream from the nonlinear medium.

The first step in the investigation of PDC of x rays into optical radiation is to measure the spectrum of the x-ray signal by scanning the angle of the analyzer crystal. This measurement is used to characterize the dependence of the spectrum of the x-ray signal at a specific offset of the pump angle from the Bragg angle and to explore the possible range of photon energies that can be measured. As an example, Fig. 2 shows the spectrum for a pumping beam at 11 keV, where the phase-matching deviation from the Bragg angle is 43 mdeg and the deviation of the detector angle from the Bragg diffraction is -37 mdeg. The sharp peak on the left corresponds to the elastic scattering, and

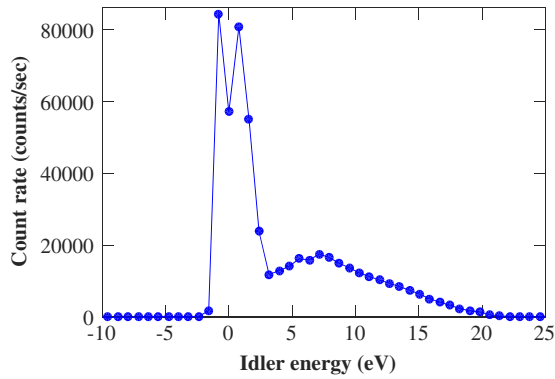


FIG. 2. X-ray signal count rate as a function of the analyzer detuning from the photon energy of the input beam. The sharp peak on the left corresponds to the elastic scattering, and the broad peak is the PDC signal (see text for further details). The solid line is a guide for the eye.

the broad peak is the PDC signal. We observe the broad PDC peak only near the phase-matching condition. The PDC peak position shifts when we vary the angles and vanishes when the angles are off the phase-matching angles. Since we measure the hard x-ray signal (at about 11 keV), and since the deepest electronic level of carbon is at ~ 280 eV, our observation cannot be attributed to x-ray fluorescence. The measured PDC spectrum corresponds to idler wavelengths (energies) in the range of about 60–400 nm (3–21 eV). Since the separation between the elastic signal and the PDC signal is pronounced, we conclude that the background reduction that the analyzer provides is adequate for the measurement of the x-ray signal of PDC into optical wavelengths. The peak is observed at 7.1 eV, where the efficiency of the PDC is the largest. This corresponds to a photon energy above the band gap of the diamond crystal, where the density of states of the valence electrons is probably the highest.

Next, to further support the evidence, we measure the dependence of the x-ray signal of the PDC process on the angular deviation from phase matching. The importance of this measurement is the ability to calculate the Fourier component of the nonlinear susceptibility from the peak of the rocking curve. Figure 3 shows the signal count rate as a function of the pump-deviation angle from the phase-matching angle. The zero of the horizontal axis corresponds to a pump deviation from the Bragg angle of 12 mdeg, which corresponds to the phase-matching angle. The photon energy is 9 keV, and the offset of the detector angle from the Bragg diffraction is 41 mdeg. The small peak on the left is the residual elastic, and the peak centered at 15 mdeg is the PDC signal. This observation of a peak, which is broader than the elastic peak but much narrower than inelastic effects, near the phase-matching condition strongly supports that the effect we observe is indeed PDC of x rays to optical wavelengths. The theoretical curve is obtained from numerical simulations based on Eq. (2), and

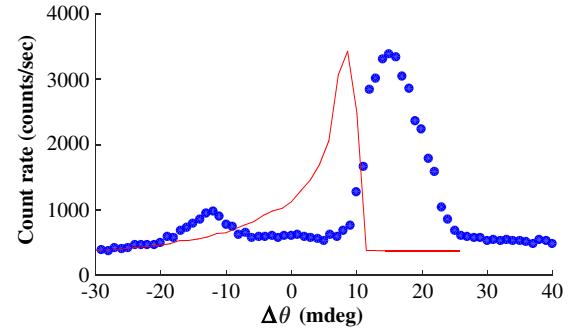


FIG. 3. X-ray signal count rate as a function of the pump-deviation angle from the phase-matching angle. The idler central wavelength is ~ 550 nm (~ 2.2 eV). The blue dots are the experimental results, and the solid red line is calculated from theory and scaled to the peak of the rocking curve.

it is normalized with respect to the experimental PDC peak by a factor of 1.24. The difference between the positions of the calculated and the measured peak, which is only 6 mdeg, is mainly because of the acceptance angle of the detector and the analyzer bandwidth (~ 1 eV), which introduce uncertainties into the values we use in our calculations. These results, together with the dependence of the density of states of the vacuum modes on the angles and frequencies, are the reasons for the deviation of the theoretical peak from the phase-matching value.

Finally, the phase-matching equations have two possible solutions for the angle of the detector, and we expect to be able to observe them experimentally. Indeed, the two solutions are clearly seen in Fig. 4, which shows the signal count rate as a function of the deviation of the angle of the detector with regards to the normal to the crystal surface from the Bragg angle (blue dots). The solid red lines are the simulations, which are obtained by using Eq. (2). The two peaks on the left and on the right of the central peak correspond to the PDC signal. The central peak is the residual elastic scattering. The deviation of the angle of the pump from the Bragg angle is 21 mdeg. The photon energy is 9 keV. The idler central energies in Figs. 4(a)–4(c) are ~ 2.2 , 3.3, and 4.4 eV, respectively. The results of the numerical simulations are scaled to the heights of the peaks of the experimental rocking curves. The ratio between the count rates of the first and the second PDC solution is smaller for higher idler energies in both the experiment and the numerical simulation, and it is a consequence of the product of the nonlinear current density and the density of states. The measured angular separation between the two solutions in panels (a) and (b) agrees remarkably with the simulations. The small difference in the angular separation between the experimental results and the simulations in panel (c) can be attributed to the bandwidth of the analyzer crystal (~ 1 eV) and to the proximity to the band gap of diamond (~ 5.5 eV), which is not considered in our theory.

The measured efficiency is proportional to the absolute square of the Fourier component of the nonlinear

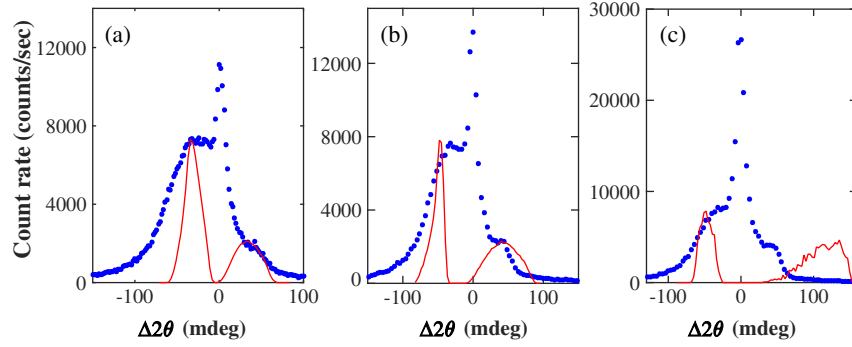


FIG. 4. X-ray signal count rate as a function of the deviation of the detector angle from the residual elastic wave for various idler center photon energies: (a) 2.2-eV idler (~ 550 nm), (b) 3.3-eV idler (~ 400 nm), and (c) 4.4-eV idler (~ 300 nm). The blue dots are the experimental results. The narrow peaks at the center in each of the panels correspond to the residual elastic wave. The peaks to the left and right correspond to the x-ray signal of the PDC for the two solutions of the phase-matching equations. The zero is the angle of the residual elastic wave. The solid red lines are calculated from theory and scaled to the peaks of the rocking curves.

susceptibility, which corresponds to the selected reciprocal lattice vector. We estimate the Fourier component corresponding to the reciprocal lattice vector normal to the C(220) atomic planes of the nonlinear susceptibility by fitting the results of the numerical simulations to the heights of the peaks of the curves in Figs. 3 and 4(a). After subtracting the DC component of the PDC rocking curve, we find that the nonlinear susceptibility for an idler energy of ~ 2.2 eV (~ 550 nm) is $\chi_{(220)}^{(2)} = 2 \times 10^{-17}$ m/V. The nonlinear susceptibility is calculated using the relation $\chi^{(2)} = -0.5ik/\epsilon_0 \sqrt{[\cos\theta_s \cos\theta_i (c\epsilon_0)^3 n_i / 2\hbar\omega_p \omega_s \omega_i]}$, where n_i is the refractive index at the idler wavelength. We note that this result is comparable to the nonlinear susceptibility $\chi_{(111)}^{(2)} = 8 \times 10^{-18}$ m/V, which was obtained in the x-ray and optical mixing experiment [with an x-ray beam at 8 keV and an optical beam at 1.55 eV (800 nm)] [6]. Since the susceptibility is proportional to the Fourier component of the charge density of the valence electrons, the measurements of the efficiencies for various reciprocal lattice vectors can be used for the reconstruction of the charge density of the valence electrons [4].

Before concluding, we discuss several important experimental aspects. We note that, while the full measurement of PDC of x rays into the optical regime should include the measurement of the optical radiation, the measurement of the x-ray photons is sufficient for retrieving microscopic information on the valence electron charge density in a manner similar to PDC of x rays into EUV [4]. In fact, for materials that are opaque at optical wavelengths, the visible radiation is not measurable. Moreover, the numerical simulations that agree with the observations of the x-ray signal predict that the PDC optical idler count rate is 2 orders of magnitude weaker than the optical fluorescence we measured in the experiment (there is no x-ray fluorescence since the deepest electronic binding energy in carbon is ~ 280 eV). The expected idler count rate is much weaker

than the signal count rate because of the large ratio between the x-ray and optical wavelengths, which leads to a high ratio between the density of states of the x-ray and the density of states of the optical wavelengths. In addition, the optical radiation is highly suppressed by internal reflection.

Since the photon energy of the pump can be chosen to be high above the electronic resonances and since the generation and absorption rates of the optical photons are very small, the perturbation of the measured state by x rays into optical PDC is expected to be negligible. This property is essential for measurements of ground states of systems where even small quanta of absorbed light can excite or change the properties of the sample.

In conclusion, we report the observation of the x-ray signal of phase-matched PDC corresponding to optical idler photons at several wavelengths in the range of 280–650 nm. The PDC signal is well above the background, and the separation from the elastic is pronounced. The widths of the rocking curves and the absolute count rates are in agreement with theory. The deviations between the calculated and measured peak positions of the PDC x-ray signal rocking curves are within the uncertainties due to the precision of the motors and the analyzer bandwidth. Our results advance the possibility to use x rays into optical PDC as a new tool to probe microscopic valence charge densities and optical properties of materials on the atomic scale. This novel tool can be used to test and improve the understanding of condensed-matter physics.

We acknowledge the European Synchrotron Radiation Facility for provision of synchrotron radiation facilities. We thank Diamond Light Source for access to Beamline I16 (Proposal No. MT14646), which contributed to the results presented here. This work was supported by the Israel Science Foundation (ISF), Grant No. 1038/13. This research was supported by a Marie Curie FP7 Integration Grant within the 7th European Union Framework Programme under Grant Agreement

No. PCIG13-GA-2013-618118. D. B. gratefully acknowledges support from the Ministry of Aliyah and Immigrant Absorption of Israel. C. B. is supported by the Deutsche Forschungsgemeinschaft (DFG) via SFB925 (Teilprojekt A4), and is thankful for travel support by the Centre for Ultrafast Imaging (CUI) and Partnership for Innovation, Education and Research (PIER) to the ESRF and Diamond Light Sources.

* sharon.shwartz@biu.ac.il

- [1] I. Freund and B. F. Levine, *Phys. Rev. Lett.* **25**, 1241 (1970).
- [2] P. M. Eisenberger and S. L. McCall, *Phys. Rev. A* **3**, 1145 (1971).
- [3] H. Danino and I. Freund, *Phys. Rev. Lett.* **46**, 1127 (1981).
- [4] K. Tamasaku, K. Sawada, E. Nishibori, and T. Ishikawa, *Nat. Phys.* **7**, 705 (2011).
- [5] T. E. Glover, D. M. Fritz, M. Cammarata, T. K. Allison, Sinisa Coh, J. M. Feldkamp, H. Lemke, D. Zhu, Y. Feng, R. N. Coffee, M. Fuchs, S. Ghimire, J. Chen, S. Shwartz, D. A. Reis, S. E. Harris, and J. B. Hastings, *Nature (London)* **488**, 603 (2012).
- [6] K. Tamasaku and T. Ishikawa, *Phys. Rev. Lett.* **98**, 244801 (2007).
- [7] K. Tamasaku and T. Ishikawa, *Acta Crystallogr. Sect. A* **63**, 437 (2007).
- [8] K. Tamasaku, K. Sawada, and T. Ishikawa, *Phys. Rev. Lett.* **103**, 254801 (2009).
- [9] B. Barbiellini, Y. Joly, and K. Tamasaku, *Phys. Rev. B* **92**, 155119 (2015).
- [10] D. Borodin, S. Levy, and S. Shwartz, *Appl. Phys. Lett.* **110**, 131101 (2017).
- [11] E. Shwartz and S. Shwartz, *Opt. Express* **23**, 7471 (2015).
- [12] I. Freund and B. F. Levine, *Phys. Rev. Lett.* **23**, 854 (1969).
- [13] S. Shwartz, R. N. Coffee, J. M. Feldkamp, Y. Feng, J. B. Hastings, G. Y. Yin, and S. E. Harris, *Phys. Rev. Lett.* **109**, 013602 (2012).
- [14] See Supplemental Material at <http://link.aps.org/supplemental/10.1103/PhysRevLett.119.253902> for a more detailed overview of the theory, the numerical simulations, and the experimental setup.
- [15] Additional experimental and theoretical details are given in Ref. [14].
- [16] S. P. Collins, A. Bombardi, A. R. Marshall, J. H. Williams, G. Barlow, A. G. Day, M. R. Pearson, R. J. Woolliscroft, R. D. Walton, G. Beutier, and G. Nisbet, *AIP Conf. Proc.* **1234**, 303 (2010).